Wigner Transport in Magnetic Fields

M. Ballicchia, C. Etl, M. Nedjalkov, and J. Weinbub
Institute for Microelectronics, TU Wien, Gußhausstraße 27–29, 1040 Wien, Austria
e-mail: balliccia@iue.tuwien.ac.at

The use of magnetic fields for controlling and manipulating electron states is vital for solid-state quantum systems [1], [2], requiring comprehensive quantum transport models, able to treat multiple dimensions and time dependence. Models based on electromagnetic (EM) potentials depend on the choice of the gauge and thus the same holds for the particular numerical approaches. Recently, a Wigner model has been suggested [3], [4], formulated in terms of general EM fields $\mathbf{E}, \mathbf{B}$, which is thus gauge-invariant. The transport equation involves the terms $D^F(\mathbf{E})$ and $H^F(\mathbf{B})$, given by the Fourier transform $FT = \int d\mathbf{s} e^{-\frac{i}{\hbar}\mathbf{ps}}$ of the quantities $\int_{-1}^{1} d\tau \left(\mathbf{s} \cdot \mathbf{E}(\mathbf{x} + \frac{\mathbf{s}\tau}{2})\right)$ and $\int_{-1}^{1} d\tau \left(\mathbf{s} \times \mathbf{B}(\mathbf{x} + \frac{\mathbf{s}\tau}{2})\right)$.

So far, there is no numerical and simulation experience with the general EM equation. In this work, we provide a first step into this direction by considering simplifying assumptions. These consider 2D transport in the $\mathbf{x} = (x, y)$ plane, an inhomogeneous magnetic field normal to the plane $\mathbf{B} = (0, 0, B(y))$ (linear along y: $B(y) = B_0 + B_1 y$), and a general electric field $\mathbf{E}(\mathbf{x})$. If $\mathbf{E}$ is stationary it is possible to redefine the Wigner potential $V_w(\mathbf{p}, \mathbf{x})$ in terms of D^F. The thus obtained equation

$$\left(\frac{\partial}{\partial t} + \frac{\mathbf{p}}{m} \cdot \frac{\partial}{\partial \mathbf{x}} + \mathbf{F} \cdot \frac{\partial}{\partial \mathbf{p}}\right) f_w(\mathbf{p}, \mathbf{x}) = \int d\mathbf{p}' V_w(\mathbf{p} - \mathbf{p}', \mathbf{x}) f_w(\mathbf{p}', \mathbf{x}) + \frac{B_1 \hbar^2}{m} \frac{e}{12} \left(\frac{\partial^2}{\partial p_y^2} \frac{\partial}{\partial x} - \frac{\partial}{\partial p_x} \frac{\partial}{\partial p_y} \frac{\partial}{\partial y}\right) f_w(\mathbf{p}, \mathbf{x}) \,, \quad (1)$$

resembles the common Wigner equation, except the additional terms originating from H^F. On the left is the force-less Liouville operator (Lo), now completed by the magnetic Lorentz force $\mathbf{F} = \frac{e}{m}\mathbf{p} \times \mathbf{B}(y)$. The third row involves higher order mixed derivatives and vanishes with $B_1 \to 0$. The force-less Lo of the standard theory in conjunction with the Wigner potential gives rise to interference, nonlocality, tunneling, negativity, and oscillatory behavior of f_w: Despite that Lo involves 'classical' Newtonian trajectories the evolution is fully coherent. In contrast, in equation (1) (i) the trajectories are driven by the inhomogeneous magnetic field $B(y)$, which modifies the interplay with V_w, and (ii) a B_1-dependent term exists, which interacts with both, $Lo(B(y))$ and V_w. We focus our simulation analysis on (i): A choice of a small B_1 allows to neglect the last term in (1) and considers the interplay between $Lo(B(y))$ and V_w in the process of magnetotunneling. A minimum uncertainty Wigner state is injected at the bottom towards a $0.3eV$ and $1nm$ barrier at $y = 30nm$. We consider four cases of (B_0, B_1): $(0, 0)$, $(-6T, 0)$, $(-6T, 0.2T/nm)$, and $(-2T, -0.2T/nm)$ (Fig. 1-4). The electron can tunnel into the upper half of the domain. The mean densities follow the classical paths (indicated lines) in accordance with the Ehrenfest theorem. In Fig. 1 the density shows a fine oscillatory structure above the barrier. The latter is destroyed by the constant magnetic field as shown in Fig. 2, which bends the mean path to a particular position. In Fig. 3, the magnetic field changes it's direction after the barrier, giving rise to a 'snake' type of evolution. Besides, the fine structure of the density above $y = 30nm$ is recovered. Observing that the magnetic field is zero around the barrier as in Fig. 1, we associate this effect with the existence of a local interplay with the EM fields. Indeed, in Fig. 4, when $B(y)$ around the barrier is particularly large (similar to case 2), the oscillations are again suppressed. The comparison of the four cases, Fig. 5, confirms this conclusion. Despite that in Fig. 4 the electron is guided to the same position as in Fig. 2, the effect on f_w is very different. This is shown by the negativity (Fig. 6), which increases with the magnitude of the magnetic field already far before the barrier. This suggests another, nonlocal effect of the interplay of the EM fields.

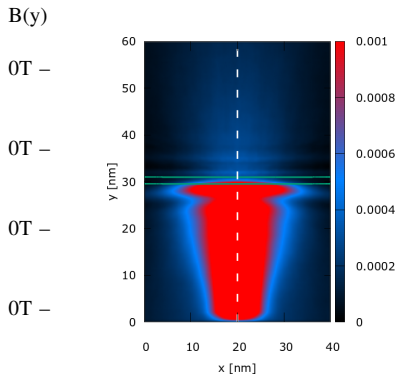

Fig. 1. Case 1: The steady-state electron density $n(x, y)$, obtained after $\mathbf{p}$ integration of f_w, is symmetric and shows a fine oscillatory structure above the barrier. A Wigner state (electron) with a kinetic energy $0.1eV$ and $\sigma_{x,y} = 3nm$ is injected at the bottom, evolving towards $+y$-direction. Dashed line indicates the mean path of the state's evolution. No magnetic field is applied (see $B(y)$ indicators on the left). Green lines indicate the barrier.

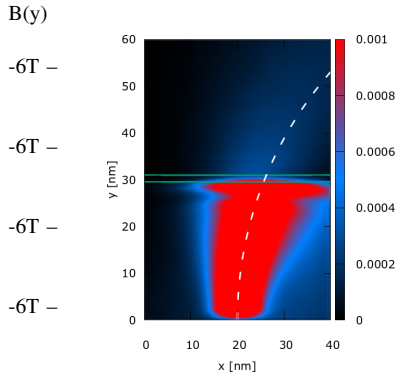

Fig. 2. Case 2: A constant magnetic field bends the density and thus the mean path.

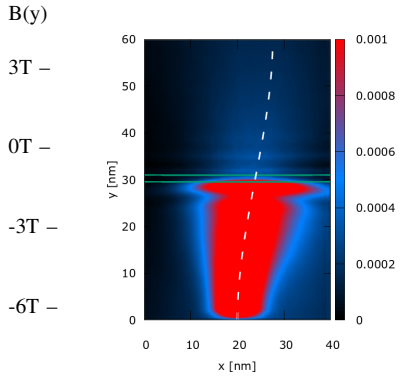

Fig. 3. Case 3: The magnetic field becomes zero at the barrier and switches the sign, giving rise to a snake type of evolution. The density in the upper half of the domain shows again a fine oscillatory structure.

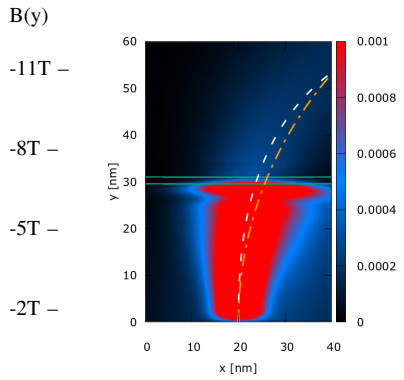

Fig. 4. Case 4: The magnetic field is gradually increased towards $+y$-direction and is particularly large at and above the barrier. The magnetic field suppresses the oscillations of the density, similar to case 2 (Fig. 2). This is confirmed in Fig. 5. The mean path (white dashed line) is compared to the mean path of case 2 (orange dot-dashed line): Although they differ, they both guide the state to the same final position.

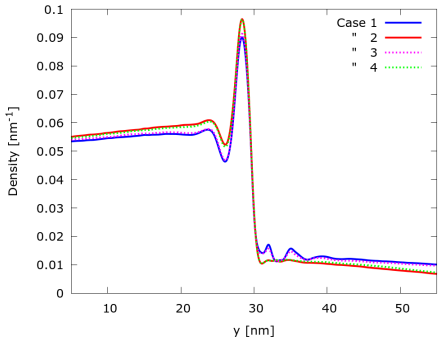

Fig. 5. Density distribution along y-direction, obtained after x-integration of $n(x, y)$: Cases 1&3 and 2&4 clearly group together, suggesting that the oscillations are suppressed in the presence of a magnetic field in the region of the barrier, further indicating that the EM fields interact locally.

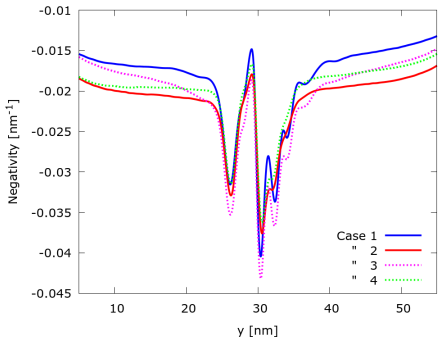

Fig. 6. Negativity obtained after integration of the quantity $f_w\theta(-f_w)$ (θ Heaviside function) on $\mathbf{p}$ and x: The negativity of f_w indicates quantum behavior. The appearance of negative values after the injection of the entirely positive initial state below the barrier ($y < 25nm$) demonstrates the nonlocal action of the barrier already without magnetic field. The negativity increases with the increase of $B(y)$ in this region, which suggests again a nonlocal interplay of the EM fields.

References

[1] P. Hoodbhoy, J.Phys.Condens.Mat. **30**, 185303 (2018).
[2] P. Mondal *et al.*, Phys.Rev.B **98**, 125303 (2018).
[3] M. Nedjalkov *et al.*, Phys.Rev.B **99**, 014423 (2019).
[4] M. Nedjalkov *et al.*, Phys.Rev.A **106**, 052213 (2022).

Acknowledgment: The financial support by the Austrian Science Fund (FWF): P33609 is gratefully acknowledged. The computational results have been achieved using the Vienna Scientific Cluster (VSC).